

Effects of Thermally Induced Configuration Changes on rAAV Genome's Enzymatic Accessibility

Yinxia Xu,^{1,6} Ping Guo,^{1,6} Junping Zhang,² Matthew Chrzanowski,³ Helen Chew,³ Jenni A. Firman,⁴ Nianli Sang,⁵ Yong Diao,¹ and Weidong Xiao²

¹School of Biomedical Science, Huaqiao University, Quanzhou, China; ²Herman B Wells Center for Pediatric Research, Indiana University, Indianapolis, IN 46202, USA; ³Temple University Medical School, Philadelphia, PA 19140, USA; ⁴United States Department of Agriculture, Agricultural Research Service, Eastern Regional Research Center, Wyndmoor, PA 19038, USA; ⁵Department of Biology, College of Arts and Sciences, Drexel University, Philadelphia, PA 19104, USA

Physical titers for recombinant adeno-associated viral (rAAV) vectors are measured by quantifying viral genomes. It is generally perceived that AAV virions disassemble and release DNA upon thermal treatment. Here, we present data on enzymatic accessibility of rAAV genomes when AAV virions were subjected to thermal treatment. For rAAV vectors with a normal genome size (≤ 4.7 kb), thermal treatment at 75°C–99°C allowed only ~10% of genomes to be detectable by quantitative real-time PCR. In contrast, greater than 70% of AAV genomes can be detected under similar conditions for AAV vectors with an oversized genome (≥ 5.0 kb). The permeability of virions, as measured by ethidium bromide (EB) staining, was enhanced by thermal stimulation. These results suggest that in rAAV virions with standard-sized genomes, the capsid and DNA are close enough in proximity for heat-induced “crosslinking,” which results in inaccessibility of vector DNA to enzymatic reactions. In contrast, rAAV vectors with oversized genomes release their DNA readily upon thermal treatment. These findings suggested that the spatial arrangement of capsid protein and DNA in AAV virions is genome-size dependent. These results provide a foundation for future improvement of vector assays, design, and applications.

INTRODUCTION

Adeno-associated virus (AAV) is a single-stranded DNA (ssDNA), non-enveloped virus of the Parvoviridae family and Dependovirus genus. It is characterized as a 20- to 25-nm particle, carrying a genome of 4.7 kb in length. Recombinant vectors derived from AAV (rAAV) are a promising tool for delivering nucleic acid content into target tissues, showing notable potential for endpoint applications in clinical therapy for patients with genetic diseases. AAV vectors designed to carry a genome larger than the standard 4.7 kb have been tested for use in gene delivery, despite their limited vector yield and nonhomogeneous viral genomes.^{1–3}

The DNA genome in an AAV virion is surrounded by a capsid comprised of sixty proteins, including the VP1, VP2, and VP3 proteins,

assembled in an approximate ratio of 1:1:10;⁴ the exact distribution depends on the serotype.⁵ AAV capsids are critical components to delivering genes *in vivo*. On the cellular level, capsids are involved in cell binding, internalization, and trafficking processes within host cells.^{6–8} At the systemic level, AAV capsids play a key role in the delivery process by dictating tissue tropism,^{9,10} immunogenicity,^{11,12} and transduction efficacy *in vivo*.^{13,14} Due to their importance in vector efficacy, there has been great effort in the field to bioengineer AAV capsids with the ultimate goal of refining the properties of rAAV vectors to promote more favorable interactions with the host. Researchers have addressed this aim with emphasis on screening AAV capsid libraries to identify new serotypes that exhibit performance at an equivalent, or higher level, than the currently used serotypes in cell or tissue applications.^{15–18}

Specific attention has also been directed toward understanding the biophysical properties of AAV capsids. The thermal stability of AAV particles has been the subject of recently published studies, which is imperative to AAV genome stability both *in vitro* and *in vivo*.^{19–22} Studies have shown that capsid stability is notably preserved in temperatures of 4°C–55°C and a pH ranging from 5.5 to 8.5.²³ This stability is maintained in the face of interactions with human or mice serum, as well as nonorganic materials, like glass, polystyrene, polyethylene, polypropylene, and stainless steel.²⁴ Additionally, studies employing electron microscopy (EM), atomic force microscopy (AFM), and fluorometric assays have demonstrated that the biophysical and ultrastructural properties of the AAV capsid fluctuate with thermal changes in a given setting.^{21,25,26} Other recent studies have indicated that AAV capsid stability may vary by serotype

Received 20 May 2020; accepted 3 June 2020;
<https://doi.org/10.1016/j.omtm.2020.06.005>.

⁶These authors contributed equally to this work.

Correspondence: Weidong Xiao, PhD, Herman B Wells Center for Pediatric Research, Indiana University, 1044 W. Walnut St., R4-121, Indianapolis, IN 46202, USA.

E-mail: xiaow@iu.edu

Correspondence: Yong Diao, PhD, Center of Molecular Medicine, Huaqiao University, No. 269, Chenghua North St. Fengze, Fujian, Quanzhou 362021, China.

E-mail: diaoyong@hqu.edu.cn



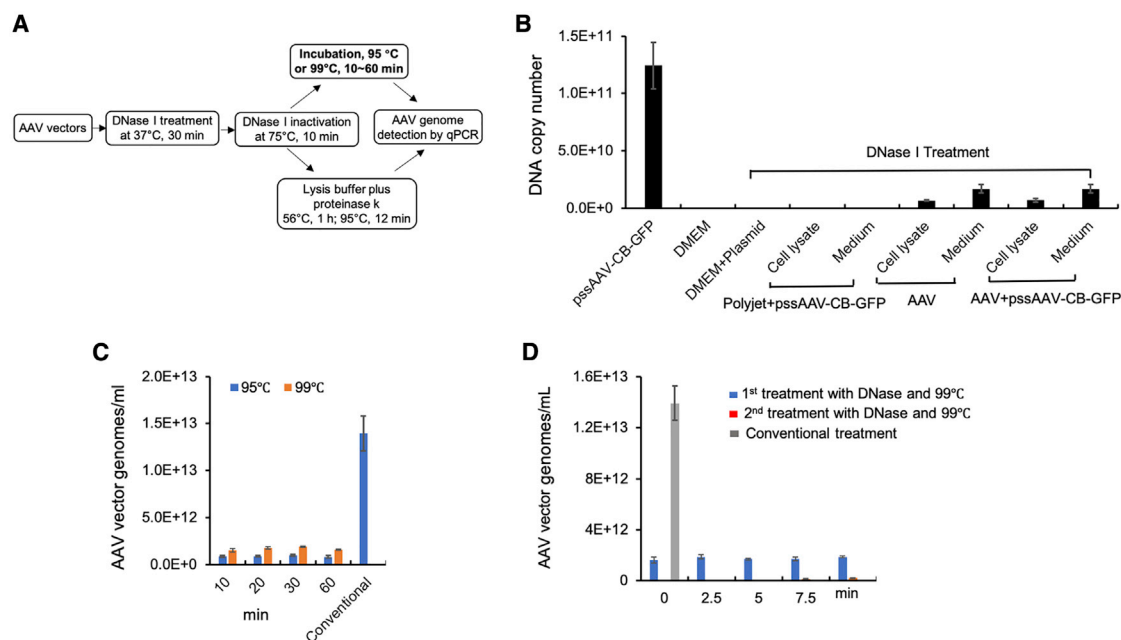


Figure 1. Evaluation of the Thermostability of AAV2-GFP Preparations

(A) Outline of experimental procedures for thermal treatment of AAV vectors, followed by genome detection via quantitative real-time PCR. (B) Assessment of the efficacy of DNase I treatment. Plasmids pssAAV-CB-GFP and AAV production helpers were transfected to 293 cells using PolyJet and incubated for 72 h before they are harvested for the assay. pssAAV-CB-GFP is the DNA standard. DMEM is the mock control without vector DNA. DMEM + plasmid is mock media spiked with standard DNA and treated with DNase I. Harvested cell lysate and medium, which are transfected with only PolyJet plus standard pssAAV-CB-GFP, are treated with DNase I. Harvested cell lysate and medium with AAV vector DNA are treated with DNase I. Harvested cell lysate and medium with AAV vector DNA are spiked with the standard pssAAV-CB-GFP and treated with DNase I. This result showed that all plasmid DNAs are completely eradicated by DNase I digestion. (C) The number of AAV2-GFP particles per milliliter uncoated during heating for 10~60 min at 95°C or 99°C, as detected by quantitative real-time PCR assay. (D) Stability of thermal-treated AAV-capsid complex. AAV particles were initially treated at 99°C and then incubated with DNase I to remove released DNA. The resulting DNA-capsid complex was then heat treated again at 99°C, and the released DNA was quantitative real-time PCR quantified. The y axis shows the amount of DNA resulting from the heat-treatment time. The data are presented with as mean \pm SD.

and the nature (single stranded or double stranded) and length of the vector DNA packaged inside.^{19,21,25} However, it has also been suggested that AAV vector stability was governed by VP3 alone, primarily due to its ratio of basic/acidic amino acids, and was independent of VP1 and VP2 or the genome packaged.²⁰ This apparent discrepancy in the findings might originate from the variance in measurement methods utilized, and it remains unclear how these physical measures relate to the biological properties of the viral particles.

In the current study, we explored enzymatic accessibility of the AAV genome upon thermal treatment utilizing quantitative real-time PCR and ethidium bromide (EB) staining. Through this, we attempt to gain further understanding on the relationship between the AAV capsid and its genome, as influenced by the condition of thermal treatment, and to provide more information on the biophysical characteristics of AAV.

RESULTS

The AAV Capsid Protects the Viral Genome from Release upon Thermal Induction

Heat denaturation of AAV vectors is a common method for releasing AAV genomes to use in subsequent assays. In previously reported

studies, AAV capsids were found to undergo ultrastructural transitions and permeability changes in response to transient heating.^{25,27,28} The approaches used in these studies were adapted to further explore the impact of thermal heating on AAV DNA release from the capsid (Figure 1A). To eliminate residual plasmid contaminants from the preceding transfection, AAV2-CB (beta-actin promoter with CMV enhancer) -GFP vectors (2.4 kb) from various sources, including crude media and cell lysate, were first treated with DNase I extensively. The results demonstrated that DNase I treatment was sufficient to remove all remnants of plasmid DNA, and any DNA detected thereafter originated solely from the AAV vectors (Figure 1B). The samples were then incubated at 95°C or 99°C over the course of 10 to 60 min and the extent of genome release assessed by quantitative real-time PCR assay. The results found that only a minority (~10%–16%) of the total vectors, as measured through employing a lysis and proteinase K digestion step to ensure the release of all genomes, could be detected (Figure 1C). To confirm that heat-denatured AAV capsids prevented the DNA genomes from detection by quantitative real-time PCR and not that the capsid had simply prevented the release of DNA, the samples analyzed in Figure 1C were subjected to another round of DNase I treatment, and then the remaining capsid was treated with additional heat

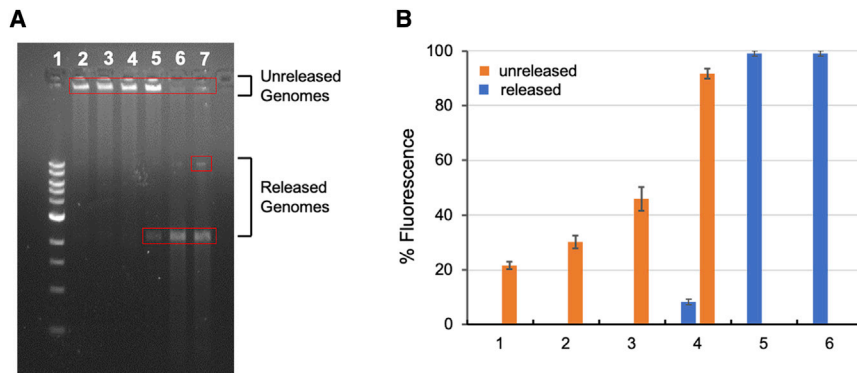


Figure 2. Characterization of AAV2-GFP Particles Following Thermal Treatment

(A) Agarose gel electrophoresis of AAV2-GFP particles. AAV vectors, treated under varying temperature for 10 min, were loaded to 1% agarose gel in Tris-acetate-EDTA (TAE) buffer and separated by electrophoresis in the presence of ethidium bromide. Lane order, lane 1: DNA marker; lane 2: untreated AAV; lanes 3–5: 55°C-, 65°C-, and 75°C-treated AAV; lane 6 (75°C + lysis buffer): 75°C in the presence of lysis buffer; lane 7 (control): AAV treated at 75°C in the presence of lysis buffer and incubated with proteinase K digestion. (B) Quantitation of observed fluorescence of DNA bands representing released or unreleased genomes shown in (A). Lane 5 represents total AAV genome. The data are presented with as mean \pm SD.

denaturation. As presented in Figure 1D, further thermal treatment failed to release additional significant amounts of vector genomes. Only less than 2% of the total vectors were detected upon the second round of heat treatment.

To confirm that the genomes remained associated with the AAV capsids following heat denaturation, AAV vectors treated at varying temperatures were subjected to agarose gel electrophoresis and the vector genomes detected by EB. In this analysis, AAV genomes released from the capsid migrated normally in the gel, and the vector DNA associated with the capsid migrated more slowly, which resulted in two distinct band (Figure 2A). The bands located at the point of origin represent unreleased genomes associated with the capsid and the permeability of the AAV capsid, whereas the downstream bands are genomes that have been released from their capsids. Only at the higher exposure temperature of 75°C does the DNA of released genomes become visible, with 8.3% of the total genome being released (Figures 2A and 2B). The amount of vector genomes shown at the origin of the gel suggested that the permeability of the AAV capsid to EB conspicuously increased from 21.7% to 91.6% along a temperature gradient from 55°C to 75°C (Figures 2A and 2B). These results demonstrate that AAV capsids exposed to thermal treatment have enhanced permeability. This allows small molecules, such as EB, to enter and bind DNA inside the capsid despite retention of overall capsid integrity, which hinders detection via quantitative real-time PCR.

Effects of the Capsid Serotype Show Varying Vector Genome Release Following Heat Treatment

To determine if thermal stability was serotype dependent, rAAV, based on serotype AAV1, -2, -5, -8, and -9, was heat treated at 75°C and 95°C and the vector genomes released quantified by quantitative real-time PCR (Figure 3). For all AAV serotypes assessed, only a small portion of the total genomes were detected, ranging from 0.07% to 9.75% at 75°C and 2.47% to 13.2% at 95°C, respectively. For AAV2, 10%–13% of the genomes were detectable by quantitative real-time PCR assay. In contrast, very few AAV8s were detected upon 75°C treatment and only 2.5% genomes detected after heat treatment at 95°C. Other serotypes showed varying results following heat treat-

ment. The results indicate that the majority of vector genomes are not accessible for quantitative real-time PCR detection for all serotypes tested. However, different capsids exhibited varying differences in the amount of vector genomes that become accessible upon exposure to heat treatment.

Vector Genome Size Affects DNA Release Following Thermal Treatment

The packaging capacity of AAV vectors has been thoroughly characterized.^{29–33} Numerous studies have demonstrated successful transduction of cells by oversized AAV vectors.^{34–36} To assess the thermal profile of AAV vectors with an oversized genome, rAAVs carrying genomes of 5.0–5.2 kb were made and analyzed. The results found that the percentage of genomes detected out of total vectors increased with genome length (Figure 4). For a genome size of 5.0, 68.8% of vectors were detected after treatment at 75°C and increased to 70.4% after treatment at 95°C. For a genome size of 5.1, 82.5% of vectors were detected after treatment at 75°C and increased to 92.7% after treatment at 95°C. For a genome size of 5.2, 87.3% of vectors were detected after treatment at 75°C and increased to 98.1% after treatment at 95°C (Figures 4A and 4B).

Next, capsid permeability of oversized vectors undergoing heat treatment was assessed using an agarose gel assay (Figures 4C and 4D). The vector DNA of AAV-5.0 kb treated at 55°C–65°C mostly remained at the top of the gel, showing no obvious DNA release from the virion. For AAV-5.1 kb and AAV-5.2 kb, free migrating DNA started to become visible even after heat treatment as low as 50°C. The quantification of DNA released is shown in Figures 4D–4F. For AAV-5.0 kb, the maximal released genome was approximately 36.2% at 75°C, which was similar to the larger vectors, AAV-5.1 kb (36% at 50°C) and AAV-5.2 kb (41% at 50°C). These results suggest that compared to AAV capsids containing normal-sized genomes, capsids carrying oversized genomes are significantly less protective.

DISCUSSION

Capsid stability has a direct association with the AAV-uncoating process, in which AAV releases its genome once inside the host cell.^{37–39} In addition to ambient pH and the composition of the buffer solutions

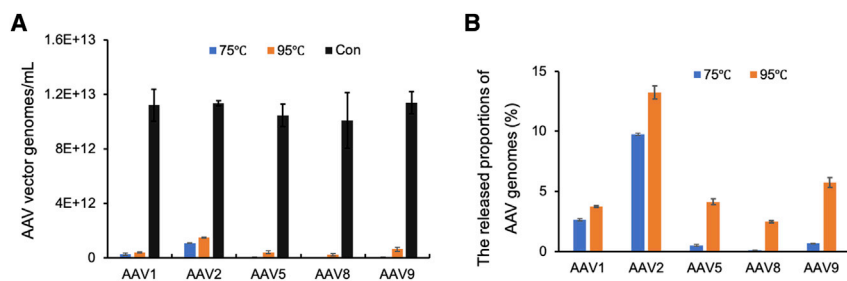


Figure 3. Evaluation of the Genome Accessibility of Various AAV Serotypes under Heat Treatment

(A) The number of AAV-GFP particles per milliliter released after heating for 10 min at 75°C or 95°C, as detected by quantitative real-time PCR assay. (B) The percentage of AAV-GFP particles uncoated after thermal treatment. The total possible number of genomes released was defined by vectors treated with a lysis buffer along with proteinase K digestion. The data are presented with as mean \pm SD.

used to store AAV vectors, temperature is another important factor affecting capsid stability.²⁴ Studies have found that pH-dependent protease activation sites exist on the AAV capsids, making capsid proteins sensitive to pH induction, with significant autocleavage occurring at pH 5.5.^{40,41} Although the optimal packaging capacity of rAAV is 4.7 kb, an oversized genome can be packaged up to a limit of 5.3 kb.²⁸ Vector genome size also affects AAV stability.

In the current study, the primary goal was to assess the vector DNA enzymatic accessibility following heat treatment. Although this is related to vector stability, it is different in that the denatured/disintegrated capsids may not have biological activities yet remain associated with the vector DNA restricting enzymatic accessibility. In standard-sized AAV particles, exposure to thermal stress under 75°C only resulted in less than 10% of total vector genomes to be detected by quantitative real-time PCR. When the temperature was raised to 95°C, the number of detectable genomes increased slightly to 16%. These results are consistent with the reported amount of linear ssDNA ejected from mostly intact capsids, as described by Bernaud et al.²¹ On the other hand, the accessibility of vector DNA is not an issue since all vector genomes can be released by the treatment of a lysis buffer along with proteinase K digestion. This result also suggests that the majority of vector genomes are shielded by the capsid, even after heat denaturation as high as 95°C.

A few methods have been used to assess thermal stability, such as antibody binding, differential scanning calorimetry (DSC), differential scanning fluorimetry (DSF), and EM. All of these methods monitored capsid disintegration. With the use of DSF, DSC, and EM, AAV2 and AAV8 melting temperature (T_m) was determined to be \sim 68°C and 71°C.^{19,20,24,42,43} With the use of antibody binding and DNase/quantitative real-time PCR, the transition temperature of AAV2 and AAV8 was determined to be between about 55°C to 70°C,⁴⁴ whereas the EM and SYBR Gold method showed a transition between 40°C and 70°C.²⁵ The combination of DNase I treatment and quantitative real-time PCR found for several AAV derivatives a dissociation temperature (T_d) of \sim 56°C. With the use of AFM, more than 60% of DNA in AAV8 was shown to be linearly ejected at 75°C, and 30% of virions were a ruptured particle.²¹ Although these methods observed the perturbation of the intact capsid particle, they did not assess vector genome enzymatic accessibility quantitatively. These methods, in combination with the enzymatic accessibility analysis in this study, allow us to have a better understanding of the arrangement of the viral capsid and its DNA content.

The DNA enzymatic accessibility of oversized AAV particles (5.0–5.2 kb) upon heat denaturation was considerably better than the standard-sized AAV vector, reaching approximately 69%–87% at 75°C and 70%–98% at 95°C by quantitative real-time PCR assay. These results demonstrate a correlation between genome size and the AAV capsid following thermal treatment. As revealed by EB staining, the permeability of the AAV capsid became further enhanced as the magnitude of thermal stimuli increased. Horowitz et al.²⁵ used computational modeling of internal capsid pressure and genome organization to explain the reverse relationship between the AAV capsid thermal stability and genome size. The accessibility of the denatured AAV genome is consistent with the vector thermal stability.

The main use of heat denaturation of AAV vectors is to measure vector titer using quantitative real-time PCR. Inaccessibility of heat-treated virion undoubtedly is the main source of systemic error, yet previous studies did not consider this issue. For example, in a previous reported study,^{44,45} heat-treated vectors are assumedly deemed 100% accessible by quantitative real-time PCR and used as the basis for the subsequent data analysis. Although this would not change the overall conclusion for these particular studies, it does indicate that the total amount of vector was underestimated. This is supported by the fact that alkaline lysis buffer plus proteinase K digestion released more vectors that were detected by quantitative real-time PCR (Figure 2).

Based on the results of this study, we proposed a model relating the state of the capsid proteins and its DNA content upon heat stimulation, which is summarized in Figure 5. The key point is that the capsid protein, albeit denatured, may still be associated with vector DNA. The resulting “heat crosslinked” product is rather stable and permeable to the small molecules, such as DNA dye. However, they are inaccessible to common enzymes, such as thermostable polymerases, used in the DNA assay. It reflects a special DNA and capsid protein arrangement in the virion.

MATERIALS AND METHODS

Virus Production and Purification

AAV vectors were generated using the triple-plasmid cotransfection method. Plasmids for pssAAV-CB-EGFP (2.4 kb), pssAAV-CB-GFP-XhoI (4.3 kb), pssAAV- β -actin-hF8-5p (5.1 kb), and pssAAV- β -actin-hF8-5p inserted with a synthesized 100-bp (5.2-kb) fragment were packaged in AAV vectors as described previously.^{46,47} Briefly, AAV helper plasmids for serotype 1, 2, 5, 8, or 9, p Δ 6 helper, and

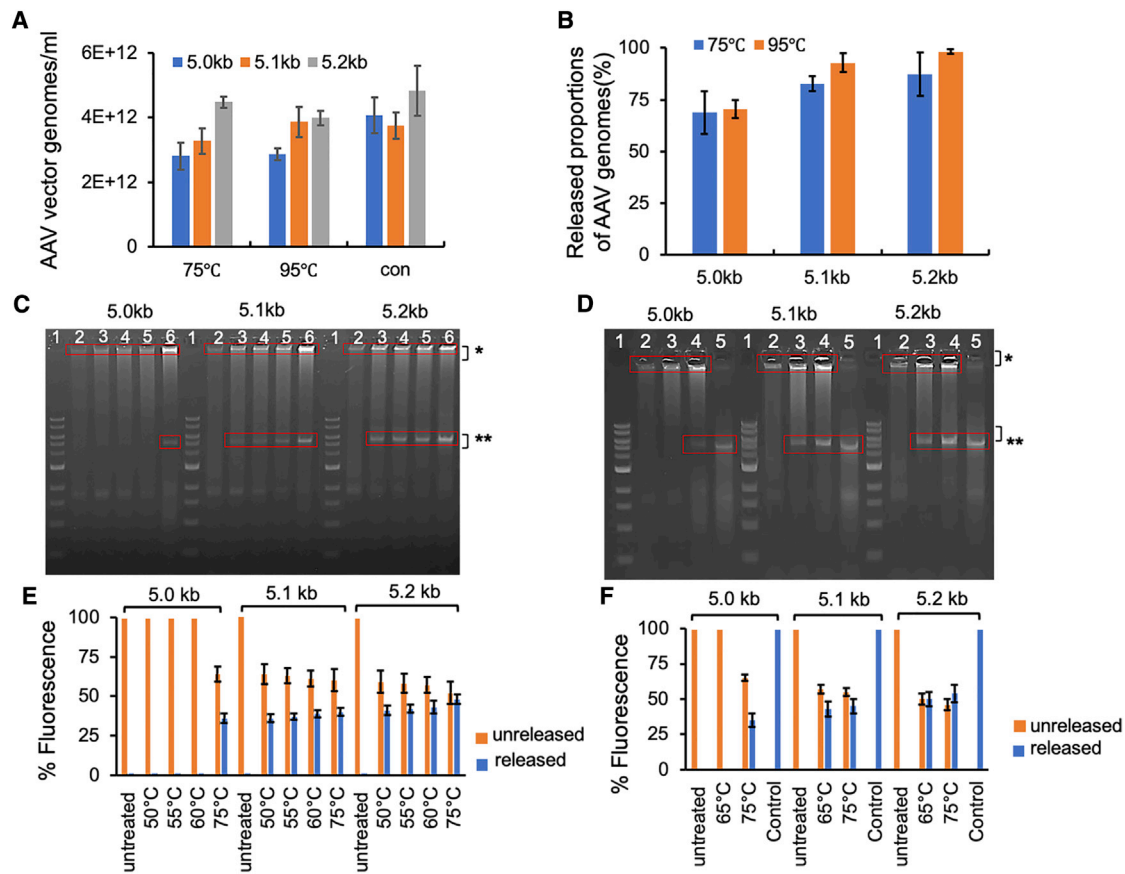


Figure 4. Evaluation of the Thermal Stability of Oversized Genome AAV Preparations

(A) The number of AAV8-factor VIII (FVIII) particles per milliliter released after heating for 10 min at 75°C or 95°C, as detected by quantitative real-time PCR assay. (B) The percentage of AAV8-FVIII particles released during hyperthermal treatment. The total possible number of genomes released was defined by vectors treated with a lysis buffer and proteinase K digestion. (C). Agarose gel electrophoresis of AAV particles following thermal treatment at 50°C, 55°C, 60°C and 75°C. (D). Agarose gel electrophoresis of AAV particles following thermal treatment at 65°C, 75°C. The control is AAV treated with proteinase K digestion. In respective order, (C) lanes 1–6: marker, untreated, 50°C, 55°C, 60°C, and 75°C and (D) lanes 1–5: marker, untreated, 65°C, 75°C, and control. *Unreleased genomes; **released genomes. (E). Quantitation of observed fluorescence of DNA bands representing released or unreleased genomes showing in (C). (F). Quantitation of observed fluorescence of DNA bands representing released or unreleased genomes showing in (D). The data are presented with as mean \pm SD.

the transgene plasmids were cotransfected into HEK293 cells at a 1:1:1 ratio and cultured in roller bottles. The vectors in transfected cells and culture media were harvested 72 h post-transfection and purified by two rounds of CsCl gradient ultracentrifugation and then extensively dialyzed against phosphate-buffered saline (PBS; NaCl 137 mM, KCl 2.7 mM, Na₂HPO₄ 10 mM, KH₂PO₄ 1.8 mM, pH 7.2) containing 5% D-sorbitol. Vector genome titers were determined by silver-stain assay and additionally verified by quantitative real-time PCR with vector titers expressed as vector genomes/milliliter, as described previously.^{48,49}

Quantitative Real-Time PCR Assay for Detection of Thermally Induced Genome Release

Viral vectors (1×10^{10} vector genomes, 1 μ L) in DNase solution containing DNase I (1 U/mL) were incubated for 30 min at 37°C, adding 1 μ L of 0.5 M EDTA (to a final concentration of 5 mM), and subsequently heated for 10 min at 75°C to cease DNase I activity. Control

samples each received lysis buffer containing proteinase K (40 μ g/mL), then were incubated for 1 h at 56°C, and finally heated for 10 min at 95°C. The samples intended for thermal treatment were directly heated following heat inactivation of DNase I treatment at the indicated temperatures. The copy numbers of viral genomes subsequently released were quantified by real-time PCR and expressed in vector genomes/milliliter. The primers used are targeting the GFP gene, forward 5'-TGACCCTGAAGTTCATCTGC-3', reverse 5'-GAAGTCGTGCTGCTTCATGT-3'; and the F8 gene, forward 5'-CACCCTGATGGTGTTCCTTTG-3', reverse 5'-GCCTGATGTATCTGCAATG-3'.

Agarose Gel Assay for Visualization of Thermally Induced Genome Release

For control group, the sample was treated according to conventional protocol: viral vectors (1×10^{11} vector genomes, 10 μ L) in DNase

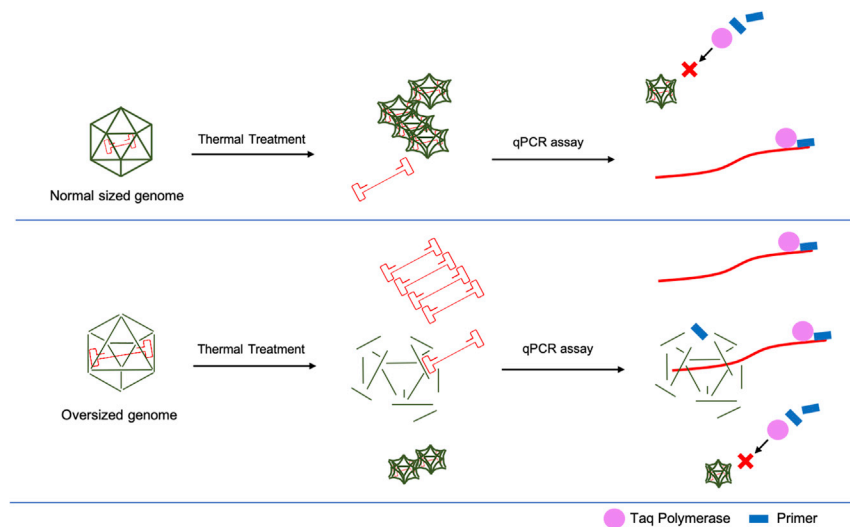


Figure 5. A Hypothetical Model for AAV Genome DNA under Thermal Treatment

Upon heat treatment, normal-sized AAVs mostly have a majority of vector DNA associated with vector capsid, which is not accessible by quantitative real-time PCR assay. In contrast, heat treatment of the oversized AAV vectors allows the majority of AAV genomes to be assayed by quantitative real-time PCR assay. The denatured AAV particles, even though they may not have biological activity, are in a special configuration in which the DNA may not be accessible enzymatically.

solution containing DNase I (1 U/mL) were incubated for 30 min at 37°C, adding 1 μ L of 0.5 M EDTA (to a final concentration of 5 mM), and subsequently heated for 10 min at 75°C to cease DNase I activity. Subsequently, the viral vectors were exposed to lysis buffer containing proteinase K (40 μ g/mL), then incubated for 1 h at 56°C, and finally heated for 10 min at 95°C. For experiment groups, the equal amounts of viral vectors (1×10^{11} vector genomes, 10 μ L) were directly heated at the indicated temperatures 50°C, 55°C, 60°C, 65°C, and 75°C for 10 min. Untreated vectors were set as the negative control. The amount of each AAV vector sample used for loading onto the agarose gel containing EB was adjusted to a final concentration of 0.5 μ g/mL for detection of thermally induced genome release. Images were captured with the aid of UV light, and fluorescence levels were analyzed by GelAnalyzer 2010a software. The bands detained in the wells are intact viral particles with genomes still inside, whereas the bands that migrated downward through the gel represent viral genomes released from uncoated viral particles.

Data were normalized to baseline spectra obtained prior to and after complete thermal transition to determine the ratio of uncoated particles to intact particles.

Statistical Analysis

The data are presented with as mean \pm SD. Statistical analysis was performed using Student's unpaired t test in SPSS software. A value of $p < 0.05$ was considered statistically significant.

AUTHOR CONTRIBUTIONS

W.X. and Y.D. conceived and supervised the study. Y.X., W.X., N.S., and J.Z. designed the experiments. Y.X., P.G., H.C., and J.Z. performed the experiments. Y.X., W.X., Y.D., N.S., and J.Z. analyzed the data. Y.X., W.X., M.C., J.A.F., and J.Z. wrote the manuscript.

CONFLICTS OF INTEREST

The authors declare no competing interests.

ACKNOWLEDGMENTS

This work was supported by grants from the National Institutes of Health (NIH) of United States (HL114152 and HL130871), National Natural Science Foundation of China (81371672 and 81371669), Major Project of University and Industry Cooperation in Fujian Province of China (2018Y4009 and 2019J05094), and Project of Science and Technology of Quanzhou of China (2016N006 and 2018C042R).

REFERENCES

- Nathwani, A.C., Tuddenham, E.G., Rangarajan, S., Rosales, C., McIntosh, J., Linch, D.C., Chowdhury, P., Riddell, A., Pie, A.J., Harrington, C., et al. (2011). Adenovirus-associated virus vector-mediated gene transfer in hemophilia B. *N. Engl. J. Med.* 365, 2357–2365.
- Gaudet, D., Méthot, J., Déry, S., Brisson, D., Essiembre, C., Tremblay, G., Tremblay, K., de Wal, J., Twisk, J., van den Bulk, N., et al. (2013). Efficacy and long-term safety of alipogene tiparvec (AAV1-LPLS447X) gene therapy for lipoprotein lipase deficiency: an open-label trial. *Gene Ther.* 20, 361–369.
- Pierce, E.A., and Bennett, J. (2015). The status of RPE65 gene therapy trials: safety and efficacy. *Cold Spring Harb. Perspect. Med.* 5, a017285.
- Buller, R.M., and Rose, J.A. (1978). Characterization of adenovirus-associated virus-induced polypeptides in KB cells. *J. Virol.* 25, 331–338.
- Mietzsch, M., Pénez, J.J., and Agbandje-McKenna, M. (2019). Twenty-five years of structural Parvovirology. *Viruses* 11, 11187–11199.
- Sonntag, F., Bleker, S., Leuchs, B., Fischer, R., and Kleinschmidt, J.A. (2006). Adeno-associated virus type 2 capsids with externalized VP1/VP2 trafficking domains are generated prior to passage through the cytoplasm and are maintained until uncoating occurs in the nucleus. *J. Virol.* 80, 11040–11054.
- Girod, A., Wobus, C.E., Zádori, Z., Ried, M., Leike, K., Tijssen, P., Kleinschmidt, J.A., and Hallek, M. (2002). The VP1 capsid protein of adeno-associated virus type 2 is carrying a phospholipase A2 domain required for virus infectivity. *J. Gen. Virol.* 83, 973–978.
- Hansen, J., Qing, K., and Srivastava, A. (2001). Infection of purified nuclei by adeno-associated virus 2. *Mol. Ther.* 4, 289–296.
- Hauck, B., and Xiao, W. (2003). Characterization of tissue tropism determinants of adeno-associated virus type 1. *J. Virol.* 77, 2768–2774.
- Wu, Z., Asokan, A., Grieger, J.C., Govindasamy, L., Agbandje-McKenna, M., and Samulski, R.J. (2006). Single amino acid changes can influence titer, heparin binding, and tissue tropism in different adeno-associated virus serotypes. *J. Virol.* 80, 11393–11397.

11. Mingozi, F., and Büning, H. (2015). Adeno-Associated viral vectors at the frontier between tolerance and immunity. *Front. Immunol.* 6, 120.
12. Louis Jeune, V., Joergensen, J.A., Hajjar, R.J., and Weber, T. (2013). Pre-existing anti-adeno-associated virus antibodies as a challenge in AAV gene therapy. *Hum. Gene Ther. Methods* 24, 59–67.
13. Nonnenmacher, M., and Weber, T. (2012). Intracellular transport of recombinant adeno-associated virus vectors. *Gene Ther.* 19, 649–658.
14. Gao, G., Vandenberghe, L.H., Alvira, M.R., Lu, Y., Calcedo, R., Zhou, X., and Wilson, J.M. (2004). Clades of Adeno-associated viruses are widely disseminated in human tissues. *J. Virol.* 78, 6381–6388.
15. Körbelin, J., and Trepel, M. (2017). How to successfully screen random Adeno-associated virus display peptide libraries in vivo. *Hum. Gene Ther. Methods* 28, 109–123.
16. Ojala, D.S., Sun, S., Santiago-Ortiz, J.L., Shapiro, M.G., Romero, P.A., and Schaffer, D.V. (2018). In vivo selection of a computationally designed SCHEMA AAV library yields a novel variant for infection of adult neural stem cells in the SVZ. *Mol. Ther.* 26, 304–319.
17. Maheshri, N., Koerber, J.T., Kaspar, B.K., and Schaffer, D.V. (2006). Directed evolution of adeno-associated virus yields enhanced gene delivery vectors. *Nat. Biotechnol.* 24, 198–204.
18. Müller, O.J., Kaul, F., Weitzman, M.D., Pasqualini, R., Arap, W., Kleinschmidt, J.A., and Trepel, M. (2003). Random peptide libraries displayed on adeno-associated virus to select for targeted gene therapy vectors. *Nat. Biotechnol.* 21, 1040–1046.
19. Rayaprolu, V., Kruse, S., Kant, R., Venkatakrisnan, B., Movahed, N., Brooke, D., Lins, B., Bennett, A., Potter, T., McKenna, R., et al. (2013). Comparative analysis of adeno-associated virus capsid stability and dynamics. *J. Virol.* 87, 13150–13160.
20. Bennett, A., Patel, S., Mietzsch, M., Jose, A., Lins-Austin, B., Yu, J.C., Bothner, B., McKenna, R., and Agbandje-McKenna, M. (2017). Thermal stability as a determinant of AAV serotype identity. *Mol. Ther. Methods Clin. Dev.* 6, 171–182.
21. Bernaud, J., Rossi, A., Fis, A., Gardette, L., Aillot, L., Büning, H., Castelnovo, M., Salvetti, A., and Faivre-Moskalenko, C. (2018). Characterization of AAV vector particle stability at the single-capsid level. *J. Biol. Phys.* 44, 181–194.
22. Drouin, L.M., Lins, B., Janssen, M., Bennett, A., Chipman, P., McKenna, R., Chen, W., Muzyczka, N., Cardone, G., Baker, T.S., and Agbandje-McKenna, M. (2016). Cryo-electron microscopy reconstruction and stability studies of the wild type and the R432A variant of adeno-associated virus type 2 reveal that capsid structural stability is a major factor in genome packaging. *J. Virol.* 90, 8542–8551.
23. Snyder, R.O., and Francis, J. (2005). Adeno-associated viral vectors for clinical gene transfer studies. *Curr. Gene Ther.* 5, 311–321.
24. Gruntman, A.M., Su, L., Su, Q., Gao, G., Mueller, C., and Flotte, T.R. (2015). Stability and compatibility of recombinant adeno-associated virus under conditions commonly encountered in human gene therapy trials. *Hum. Gene Ther. Methods* 26, 71–76.
25. Horowitz, E.D., Rahman, K.S., Bower, B.D., Dismuke, D.J., Falvo, M.R., Griffith, J.D., Harvey, S.C., and Asokan, A. (2013). Biophysical and ultrastructural characterization of adeno-associated virus capsid uncoating and genome release. *J. Virol.* 87, 2994–3002.
26. Wang, J., Xie, J., Lu, H., Chen, L., Hauck, B., Samulski, R.J., and Xiao, W. (2007). Existence of transient functional double-stranded DNA intermediates during recombinant AAV transduction. *Proc. Natl. Acad. Sci. USA* 104, 13104–13109.
27. Johnson, J.S., Li, C., DiPrimio, N., Weinberg, M.S., McCown, T.J., and Samulski, R.J. (2010). Mutagenesis of adeno-associated virus type 2 capsid protein VP1 uncovers new roles for basic amino acids in trafficking and cell-specific transduction. *J. Virol.* 84, 8888–8902.
28. Kronenberg, S., Böttcher, B., von der Lieth, C.W., Bleker, S., and Kleinschmidt, J.A. (2005). A conformational change in the adeno-associated virus type 2 capsid leads to the exposure of hidden VP1 N termini. *J. Virol.* 79, 5296–5303.
29. Grieger, J.C., and Samulski, R.J. (2005). Packaging capacity of adeno-associated virus serotypes: impact of larger genomes on infectivity and postentry steps. *J. Virol.* 79, 9933–9944.
30. Hermonat, P.L., Quirk, J.G., Bishop, B.M., and Han, L. (1997). The packaging capacity of adeno-associated virus (AAV) and the potential for wild-type-plus AAV gene therapy vectors. *FEBS Lett.* 407, 78–84.
31. Dong, J.Y., Fan, P.D., and Frizzell, R.A. (1996). Quantitative analysis of the packaging capacity of recombinant adeno-associated virus. *Hum. Gene Ther.* 7, 2101–2112.
32. Allocca, M., Doria, M., Petrillo, M., Colella, P., Garcia-Hoyos, M., Gibbs, D., Kim, S.R., Maguire, A., Rex, T.S., Di Vicino, U., et al. (2008). Serotype-dependent packaging of large genes in adeno-associated viral vectors results in effective gene delivery in mice. *J. Clin. Invest.* 118, 1955–1964.
33. Lai, Y., Yue, Y., and Duan, D. (2010). Evidence for the failure of adeno-associated virus serotype 5 to package a viral genome > or = 8.2 kb. *Mol. Ther.* 18, 75–79.
34. Choi, J.H., Yu, N.K., Baek, G.C., Bakes, J., Seo, D., Nam, H.J., Baek, S.H., Lim, C.S., Lee, Y.S., and Kaang, B.K. (2014). Optimization of AAV expression cassettes to improve packaging capacity and transgene expression in neurons. *Mol. Brain* 7, 17.
35. Dong, B., Nakai, H., and Xiao, W. (2010). Characterization of genome integrity for oversized recombinant AAV vector. *Mol. Ther.* 18, 87–92.
36. Wu, Z., Yang, H., and Colosi, P. (2010). Effect of genome size on AAV vector packaging. *Mol. Ther.* 18, 80–86.
37. Thomas, C.E., Storm, T.A., Huang, Z., and Kay, M.A. (2004). Rapid uncoating of vector genomes is the key to efficient liver transduction with pseudotyped adeno-associated virus vectors. *J. Virol.* 78, 3110–3122.
38. Sipo, I., Fechner, H., Pinkert, S., Suckau, L., Wang, X., Weger, S., and Poller, W. (2007). Differential internalization and nuclear uncoating of self-complementary adeno-associated virus pseudotype vectors as determinants of cardiac cell transduction. *Gene Ther.* 14, 1319–1329.
39. Zhong, L., Li, W., Yang, Z., Qing, K., Tan, M., Hansen, J., Li, Y., Chen, L., Chan, R.J., Bischof, D., et al. (2004). Impaired nuclear transport and uncoating limit recombinant adeno-associated virus 2 vector-mediated transduction of primary murine hematopoietic cells. *Hum. Gene Ther.* 15, 1207–1218.
40. Salganik, M., Venkatakrisnan, B., Bennett, A., Lins, B., Yarbrough, J., Muzyczka, N., Agbandje-McKenna, M., and McKenna, R. (2012). Evidence for pH-dependent protease activity in the adeno-associated virus capsid. *J. Virol.* 86, 11877–11885.
41. Douar, A.M., Poulard, K., Stockholm, D., and Danos, O. (2001). Intracellular trafficking of adeno-associated virus vectors: routing to the late endosomal compartment and proteasome degradation. *J. Virol.* 75, 1824–1833.
42. Thorne, B.A., Quigley, P., Nichols, G., Moore, C., Pastor, E., Price, D., Ament, J.W., Takeya, R.K., and Peluso, R.W. (2008). Characterizing clearance of helper adenovirus by a clinical rAAV1 manufacturing process. *Biologicals* 36, 7–18.
43. Pacouret, S., Bouzelha, M., Shelke, R., Andres-Mateos, E., Xiao, R., Maurer, A., Mevel, M., Turunen, H., Barungi, T., Penaud-Budloo, M., et al. (2017). AAV-ID: A rapid and robust assay for batch-to-batch consistency evaluation of AAV preparations. *Mol. Ther.* 25, 1375–1386.
44. Murphy, S.L., Bhagwat, A., Edmonson, S., Zhou, S., and High, K.A. (2008). High-throughput screening and biophysical interrogation of hepatotropic AAV. *Mol. Ther.* 16, 1960–1967.
45. Feiner, R.C., Teschner, J., Teschner, K.E., Radukic, M.T., Baumann, T., Hagen, S., Hannappel, Y., Biere, N., Anselmetti, D., Arndt, K.M., and Müller, K.M. (2019). rAAV engineering for capsid-protein enzyme insertions and mosaicism reveals resilience to mutational, structural and thermal perturbations. *Int. J. Mol. Sci.* 20, 5702.
46. Wang, Q., Dong, B., Pokiniewski, K.A., Firman, J., Wu, Z., Chin, M.P., Chen, X., Liu, L., Xu, R., Diao, Y., and Xiao, W. (2016). Syngeneic AAV pseudo-particles potentiate gene transduction of AAV vectors. *Mol. Ther. Methods Clin. Dev.* 4, 149–158.
47. Dong, B., Duan, X., Chow, H.Y., Chen, L., Lu, H., Wu, W., Hauck, B., Wright, F., Kapranov, P., and Xiao, W. (2014). Proteomics analysis of co-purifying cellular proteins associated with rAAV vectors. *PLoS ONE* 9, e86453.
48. Hauck, B., Chen, L., and Xiao, W. (2003). Generation and characterization of chimeric recombinant AAV vectors. *Mol. Ther.* 7, 419–425.
49. Cao, L., Liu, Y., Doring, M.J., and Xiao, W. (2000). High-titer, wild-type free recombinant adeno-associated virus vector production using intron-containing helper plasmids. *J. Virol.* 74, 11456–11463.